IDENTIFICATION AND VALIDATION OF NATURAL PERIODS AND MODAL DAMPING RATIOS FOR SEISMIC DESIGN AND BUILDING CODE

Yijun Xiang, Angie Harris, Farzad Naeim, and Farzin Zareian

Department of Civil & Environmental Engineering
University of California, Irvine

Abstract

Ninety-four buildings, with a total of 1045 distinct seismic event and building direction records, were selected from the CSMIP database to identify modal quantities (i.e., natural periods and equivalent viscous damping ratios). The selected buildings include steel and reinforced concrete moment resisting frames (i.e., SMRF, and RCMRF), reinforced concrete walls (RCW), concentrically braced frames (CBF), eccentrically braced frames (EBF), masonry walls (MAW), precast concrete walls (PCW), reinforced concrete tilt-up bearing walls (RCTUW), unreinforced masonry (URM), and WOOD. Simplified and practical equations for modal quantities along with variation of such parameters to structural system types, building height, amplitude of excitation, and system identification technique for a subset of buildings were reliable data was available are presented.

Introduction

Over the past few decades, researchers have utilized modal analysis as a means to estimate the natural periods and damping ratios of structural systems. The use of equivalent damping in seismic design has been at best ambiguous and not well defined. This is a major issue for seismic design of new buildings, and retrofit of existing structures alike, because no matter what design method is implemented, an estimate of fundamental period and equivalent modal viscous damping is necessary for the structural design process. The civil engineering community has utilized experimental data from instrumented buildings and system identification to gain insight on the actual dynamic characteristics of existing buildings. Until the implementation of system identification, the estimates of these dynamic characteristics had been at best meager estimates. The following provides a succinct review of previous research in engineering assessment of structural modal properties using system identification techniques.

Natural Periods

Several researchers have utilized system identification techniques to estimate natural periods to aid in the assessment of existing buildings and to evaluate the effectiveness of existing code period formulas. Cole *et al.* (1992) estimated the natural periods of sixty-four buildings using the transfer functions of the Fourier amplitude spectrum. These building periods were then compared to the code period formulas of the 1991 Uniform Building Code–UBC-91–(UBC, 1991) and 1990 Structural Engineers Association of California (SEAOC) Blue Book (SEAOC, 1990). They concluded that in most cases, the measured periods are longer than those of the code

periods for steel and concrete moment frames, but correlate well with the upper bound period formula. In addition, the measured periods for shear walls are usually shorter than that of the code formulas. Following Cole *et al.* (1992), Goel and Chopra (1997 & 1998) performed system identification on twenty-seven Reinforced Concrete Moment Resisting Frames (RCMRF), forty-two Steel Moment Resisting Frames (SMRF), and nine Reinforced Concrete Wall (RCW) buildings to determine their natural periods in comparison with the current code formulas of the ATC 3-06 (ATC, 1978), UBC-97 (UBC, 1997), SEAOC (1996), and National Earthquake Hazards Reduction Program (NEHRP, 1994). It was determined that the code formulas for the estimation of natural periods, at that time, were inadequate and led to shorter periods for RCMRFs and SMRFs, but longer periods than that identified for RCWs. New formulas were then derived, which have continued to be the basis for the current American Society of Civil Engineers/Structural Engineering Institute (ASCE/SEI) approximate period formulas.

Similarly, Kwon and Kim (2010) evaluated the fundamental periods of RCMRF and SMRF buildings that depicted the lower bound of code formulas and the periods of RCWs were shorter than code predicted values. Hong and Hwang (2000) performed system identification with the autoregressive exogenous (ARX) model of twenty-one RCMRF buildings in Taiwan and determined that the identified periods are less than that predicted in the UBC-97. Contrary to most studies, Lee *et al.* (2000) measured the natural periods of shear wall buildings only to find that the periods determined from the code formulas are significantly less that of the measured periods. Code period formulas, as previously noted, are based on values estimated from existing buildings through system identification. The trends seen in estimated periods can be influenced by the method of estimation, type of building studied, changes in design methods and philosophy, and the ground motions used to estimate the periods. On the other hand, several studies have explored the discrepancies between the natural periods provided through finite element models (FEM) and those estimated through system identification. This discrepancy comes from the inability of engineers to capture all forms of building lateral stiffness. This additional lateral stiffness is the result of the nonstructural elements that participate in the actual building response.

Since conventional methods being used by typical engineers to estimate dynamic response do not include the participation of all sources of stiffness, several researchers have worked to create an FEM methodology that designates all known sources of stiffness for the determination of natural periods. Hatzigeorgiou and Kanapitsas (2013) modeled twenty existing buildings, incorporating the stiffness of infill walls and soil flexibility properties to determine the natural period through numerical analysis. They formulated an expression for the estimation of the natural period based on the results of the models that account for building height, building width, shear wall ratio, and subgrade modulus, providing a comparable estimate to current code formulas. Amanat and Hoque (2006) explored the dependency of building periods on the percentage and distribution of infill walls by modeling diagonal struts to represent infill walls. They refined the UBC-97 equation for the fundamental period to include building geometry and the presence of infill panels based on the computational analysis. Similarly, Kocak and Yildirim (2011) modeled varying percentages of infill walls in SAP2000, determining that there is as much as forty-five percent change in period for buildings modeled with infill as opposed to bare frames. Skolnik *et al.* (2007) utilized the subspace state space identification method (N4SID) to compare identified modal parameters to that determined through FEM analysis. It was

determined that the participation of nonstructural components caused the natural period to be shorter for ambient vibration as opposed to low-to-moderate seismic excitation. As a result, the model was updated to account for the additional stiffness and mass using a modal-sensitivity based method.

Few studies have explored to what extent the nonstructural elements contribute to the overall stiffness of a building. Poovarodom and Charoenpong (2008), and Memari *et al.* (1999) investigated the progression of the fundamental period of reinforced concrete and steel buildings (respectively) throughout various stages of construction. The same study determined that as the completion of the building progressed and the percentage of nonstructural elements increased, the fundamental period decreased; proving the significance of the nonstructural elements' contribution to the building stiffness, and subsequently the estimation of natural periods and building performance.

Damping

The evaluation of building performance is not only dependent on the accurate estimation of its natural period, but also its damping. It is necessary for the energy dissipation of a building to be accurately modeled. However, damping continues to include much uncertainty and the ratios currently used in seismic design continue to be anything but well-defined. The Minimum Design Loads for Buildings and Other Structures, ASCE/SEI 7-10 (ASCE, 2010) requires the use of %5 damping, whereas FEMA P-58-1 (FEMA, 2012) requires that equivalent viscous damping should be within the range of %1 to %5 of the critical damping for the predominant modes. Similarly, the Los Angeles Tall Buildings Structural Design Council (LATBSDC, 2014) suggests that the additional modal or viscous damping should not exceed %2.5 of the critical damping for predominant modes. It is evident that a damping value between %1 and %5 should be used; however, the respective damping values for differing Lateral Force Resisting Systems (LFRS) are not explicitly given, providing additional uncertainty into the design process.

The history of design has included the use of classical damping, Rayleigh damping, which is only based on known building mass and stiffness. As previously discussed, stiffness is not always clearly defined. Consequently, Rayleigh damping has resulted in unrealistically large and non-conservative values. Current seismic design methods use equivalent linear viscous damping to model energy dissipation. However, these linear models, like others, have proven to provide false damping values (Bernal, 1994), especially when analyzing nonlinear behavior. Furthermore, studies have estimated damping ratios of existing buildings through system identification to explore relationships between building modal parameters, such as forecast models of period and damping (Lagomarsino 1993). Although, Lagomarsino's damping formulas were based on a viscous damping model, they did not prove that structural damping is viscous in nature.

Buildings are complex and the damping of these structures cannot solely be determined from a linear model. Frictional damping must be taken into account. Wyatt (1977) introduced the term "stiction" (static friction), where non-linear range/increase in damping can be correlated to the imperfections of the material the building is comprised of, which is aligned with fracture mechanics. The imperfections in the material are mobilized when the structure is excited; thus,

dissipating energy and increasing the structural damping. Subsequently, several studies have elaborated on Wyatt's theory, choosing to estimate equivalent damping based on known seismic excitation and system identification, showing that damping is amplitude dependent, and resulting in a myriad of equations for damping (Jeary, 1997; Li *et al.*, 1999; Davenport and Hill-Caroll, 1986; Fang *et al.*, 1999). It was found that at low amplitudes, damping seems to remain constant. As the amplitude increases, damping increases as well, in a non-linear range, until it arrives at a plateau at a higher amplitude of excitation (Jeary 1997). Tamura (2008) further explored this concept and demonstrated that damping increases only until the amplitude corresponding to the critical tip ratio is reached. The corresponding amplitude to this ratio is the critical point at which the damping begins to decrease. This idea corresponds to the assumption that as the amplitude of excitation increases, friction builds until it reaches a point when the components of the structure have "slipped" and the friction is constant, causing the damping relative to the friction forces to remain constant and eventually decrease. Satake *et al.* (2003) performed an analysis of building periods and modal damping ratios obtained from a database of 137 steel-framed buildings, twenty-five reinforced concrete buildings, and forty-three steel-framed reinforced concrete buildings. First mode damping was found to decrease with natural period (increasing with natural frequency). In addition, it was determined that the damping is amplitude dependent and increasing with mode shape number. Meanwhile, the first mode damping ratios in the small excitation amplitude region increase linearly with natural frequency or vibration amplitude. Bernal *et al.* (2012) similarly concluded that damping ratios, though they contained high amount of variability, increased with natural frequency.

On the other hand, future studies have explored damping and its dependence on the dominant building response characteristics. Bentz and Kijewski-Correa (2008) discussed the prediction of damping based on the dominance of a structural systems deformation mechanisms, shear or cantilever (i.e. flexural) action. Shear deformation takes precedence in frames where they deform from its generally square nature to a shape similar to a parallelogram. Cantilever deformation usually occurs in shear wall systems and other systems where the structure behaves like a continuous cantilever and the aspect ratio of the structure aids in the determination of the level of cantilever action. It was determined that damping values are more scattered for dual systems (between the shear and cantilever-flexure condition). As systems become more cantilever, damping values decrease. This is mainly due to reduction of effective interstory drift ratio, that is, the total interstory drift ratio minus rigid rotation of the story due to cantilever action. Reduction in effective interstory drift ratio results in the reduction of energy dissipation mechanism of the story–that is mostly friction based–and consequently leads to the reduction of damping values.

Data Collection and Description

CSMIP database of instrumented buildings contains structural records from more than 561 events in the general California crustal area. For the research study presented herein, ninety-four buildings, with a total of 1045 distinct seismic event and building direction records, are selected from the CSMIP database. The selected buildings include steel and reinforced concrete moment resisting frames (i.e., SMRF, and RCMRF), reinforced concrete walls (RCW), concentrically braced frames (CBF), eccentrically braced frames (EBF), masonry walls (MAW), precast concrete walls (PCW), reinforced concrete tilt-up bearing walls (RCTUW), unreinforced

masonry (URM) and WOOD. The list of the CSMIP instrumented buildings used in this study is presented in Appendix A (Table A.1). Among the 94 buildings used in this study, there are 25 SMRF, 11 RCMRF, 30 RCW, 11 CBF, 3 EBF, 6 MAW, 3 PCW, 2 RCTUW, 1 URM, and 2 WOOD buildings with 214, 123, 380, 145, 34, 74, 40, 9, 8 and 18 distinct seismic event and building direction records. Figure 1 provides further information on the statistics of the dataset used in this study.

System Identification

Four system identification methods are used for assessing natural periods and structural damping of the dataset. These system identification methods include: (1) ERA-OKID method (Luş *et al.*, 1999), (2) SRIM method (Juang, 1997), (3) N4SID (Van Overschee & De Moor, 1994), and (4) EFDD method (Ghahari *et al.* 2014). As the estimated frequency and damping ratio vary with the selection of different System Identification method as well as the selection of parameters for system realization especially in time-domain methods such as model order, starting point, time length and etc., a combined method is adopted for identification of a unique value of frequency and damping ratio in each mode considering all possible model parameters within all three time-domain System Identification methods. In this study, model order *N* and the time length *p* which indicate the number of layers the input and output information is stacked are considered as two parameters in SRIM method; model order *N* and the time length *p* which indicate how far the Hankel matrix is truncated are considered as two parameters in ERA-OKID method; model order *N* and the time length *p* which indicate the length of projection of future output onto input and past output are considered as two parameters in N4SID method.

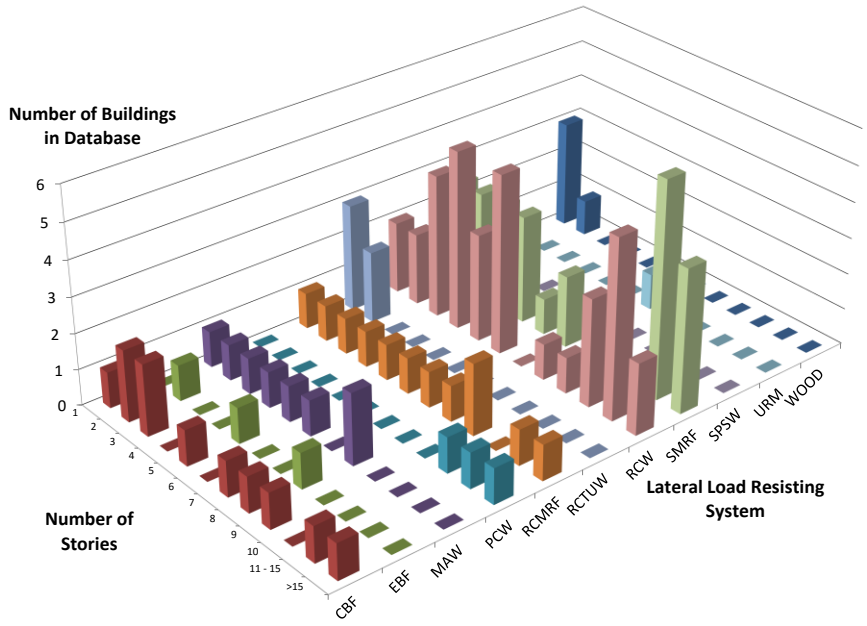

Figure 1. Statistics of the dataset used in this study

The process for combining the results of each System Identification method was developed to assure the results are encompassing and can address the variety of structural

systems in the CMSIP database. First, several combinations of model parameters are selected in each time domain method. For example, model order is selected based on the number of stories and the time length is selected based on the stability and rate of convergence of the state space model. Each specific combination of model parameters will lead to a specific estimate of frequency and damping ratio for all modes. Once a number of frequency and damping ratio estimates are obtained in each time domain method, the results are combined together after duplicating all estimates from each method based on a least common multiple of the number of estimates. The three time-domain methods are equally treated. Predominant frequencies can therefore be picked from those frequency components at peaks which represents the frequency component with the most population. Both frequency and damping ratio estimates are obtained by averaging all estimates in predominant frequency ranges. Final results are then compared to EFDD (Enhanced Frequency Domain Decomposition) estimates for verification.

To demonstrate the combination process, frequencies and damping ratios of the first three modes from the System Identification results of a 12-story SMRF building #24566 subject to the ground motion Anza 12Jun2005 with a PGA of 0.004g are shown in Figure 2. The histogram represents the population of each frequency component. Near the peaks are the mean values of frequencies and damping ratios given at the first line and the coefficients of variance given at the second line. Mode shape of each mode is plotted along with the mode shape values given at the place where sensors are implemented. Also the results obtained from combined time-domain method are compared to those obtained from EFDD (Enhanced Frequency Domain Decomposition) method for verification.

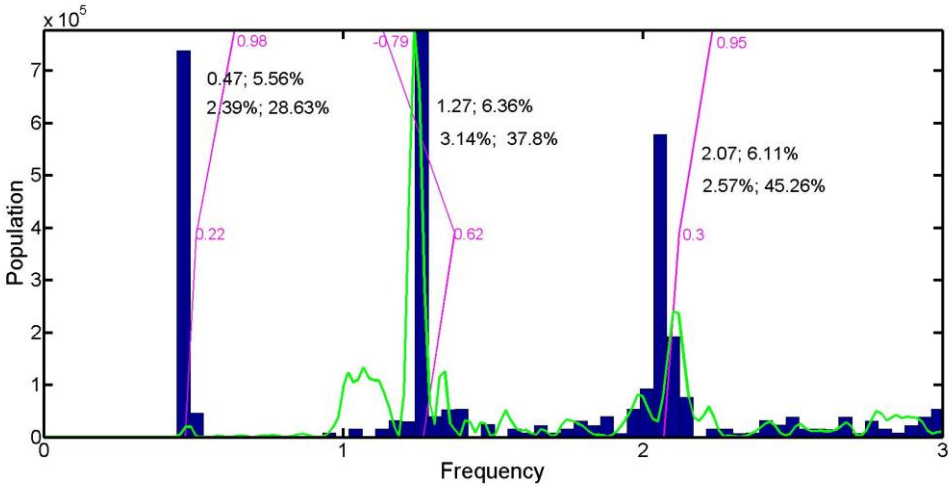

Figure 2. Frequency and damping estimates for each mode based on the combined System ID for the 12-story SMRF building #24566 subject to Anza 12Jun2005.

Equations for Natural Periods & Modal Damping Ratios for Buildings

The objectives of this study are to quantify natural periods and equivalent viscous damping ratios for buildings in the form of a set of meaningful and practical equations based on structural system types, building height and other factors that may prove to be significant. Multivariate regression analysis is utilized to fit modal properties to expressions in either linear

function or power function with building heights, building occupancy and ground motion intensity measures being considered as predictors. The goodness of fit is measured using T-tests and F-tests. In general, T-test is a test of whether an individual regression coefficient equals zero, accessing one regression coefficient at a time, while F-test accesses multiple regression coefficients simultaneously, is an overall test of whether the regression coefficients are jointly not all equal to zero. Difference between the full model and a reduced model when one or more predictors are excluded is estimated by the mean of squared errors *MSE* (sum of squared errors *SSE* divided by its degree of freedom). A *P-value* less than the significance level (usually 0.05) is considered significant, and a significant *P-value* leads to the rejection of null hypothesis and concludes that the model has better performance compared to the model with no predictors. As a measure of the goodness of regression fitting approximates data points, coefficient of determination R^2, which equals the ratio of sum of squared deviation *SSR* to total variation *SSTO*, stands for the effect of predictors in reducing the variation; the larger R^2 is, the more total variation is reduced.

Preliminary model investigation plays an important role before the modal is built. The correlation matrix is constructed to observe whether the response and each of the predictor candidates are positively or negatively correlated. Also, the correlation between predictors is indicative of collinearity. Automatic search procedure, including Best Subsets algorithm and Stepwise Regression method, serves to select the most proper set of predictors without evaluating all of the possible combinations. Five criteria for model selection are utilized: coefficient of determination; adjusted coefficient of determination which takes the total number of predictors into consideration as a penalty; mean of squared errors *MSE*, *Mallow's Cp* which compares the precision and bias of the full model with models including only a subset of the predictors; *PRESSp* which measures the sum of the squared prediction errors while a single prediction error is defined as the difference between fitted response with the deletion of a single case and the observed response. Best Subsets regression identifies the best among several models with respect to specified criterion for each number of predictors included in the model. Unlike Best Subset regression accepting several models, the forward stepwise regression develops a single model by adding or deleting a predictor variable at each step, and the criterion for adding or deleting a predictor is defined through a T-test involving the difference between model including that predictor and model excluding that predictor. The ultimate model with suitable predictors decided through model selection is then examined by hypothesis tests.

The aptness of the regression model should be examined before any inference is undertaken. Diagnostics involving residuals are considered, including tests for normality, test for constancy, test for outliers and influential cases and the lack of fit test. Two tests are employed for the examination of the normality of error terms: *Ryan-Joiner* normality test and *Kolmogorov-Smirnov* normality test.

For ascertaining the constancy of error variance, *Brown-Forsythe* test, which is independent of normality, is applied. For identification of outlying observations, as well as, influential cases, *Hat Matrix Leverage values*, *Studentized Deleted residuals*, *DFFITS* and *Cook's Distance* are calculated and the corresponding T-tests or F-tests are employed. For determining whether a specific function is a good fit for the data, F-test for lack of fit, which requires repeat cases at one or more predictors' levels, is taken up. In addition, the standardized regression model is introduced for diagnostics of lack of comparability due to differences in the

variables units and diagnostics of multicollinearity when predictor variables are correlated. Variance Inflation Factor (*VIF*) which represents the level of collinearity is also computed from the standardized model, and a large value of *VIF* is indicative of serious multicollinearity problem and then interaction terms need to be included in the model.

Remedial measures need to be carried out when diagnostics demonstrate that the regression model is not appropriate enough for the data. For non-normality of error terms, *Box-Cox Transformation* alters the shape and the spread of the distribution of response to correct the skewness of the distribution of error terms. Weighted least squares method helps to reduce unequal error variances by introducing weights into the regression, while weights are affected by the absolute residuals or squared residuals. Robust regression is taken up in the same manner if the error terms exhibit outliers and influential cases. *IRLS* robust regression is employed in this study by the use of weights that vary inversely with the magnitude of scaled residuals. Several iterations may be required to keep on revising the weights until convergence criteria is satisfied. Since predictor multicollinearity is not detected in this study, remedial techniques modifying the sampling distribution of regression coefficients to overcome multicollinearity problem, such as *Ridge* regression, is not considered.

Aside from the linear regression model that takes the logarithm of response (natural period, damping ratio) and predictors (building heights, ground motion intensity measure, etc.), nonlinear regression models involving these variables are studied for comparison purposes. In this study, the Gauss-Newton method numerically searches the solution using Taylor series expansion to approximate a nonlinear model with linear terms, and the linear model solution obtained before is selected as the nonlinear initial guess.

Modal Properties and for Steel Moment Resisting Frames (SMRF)

Dynamic properties of 25 SMRF buildings representing 195 building-events (data points) were computed using System Identification methods. Building Height ranges from 26 ft to 692.5 ft, *PGA* ranges from 0.004g to 0.299g, *PGV* ranges from 0.187cm/s to 24.404 cm/s, and *PGD* ranges from 0.008cm to 12.639cm. The buildings were divided into two subcategories as far as occupancy is concerned: (1) Residential, office and commercial buildings, (2) Hospitals. Our recommended regression equation for estimating the fundamental period, and first mode damping of SMRF buildings is given in Eq. (1), and Eq. (2), respectively; units are: T_1 (sec), *PGV* (cm/sec), *H*(ft). Comparison of regression results for fundamental period of SMRFs at *PGV* = 10cm/s and ASCE 7-10 formula are shown in Figure 3. The 95% confidence and prediction intervals for the damping regression equation are presented in Figure 4.

$$T_1 = \begin{cases} 0.017 H^{0.82} PGV^{0.06} & \text{Hospital} \\ 0.026 H^{0.82} PGV^{0.06} & \text{Other} \end{cases} \qquad \text{Eq. (1)}$$

$$\xi_1 = 8.86 H^{-0.16} \qquad \text{Eq. (2)}$$

Modal Properties and for Reinforced Concrete Moment Resisting Frames (RCMRF)

Dynamic properties of 11 RCMRF buildings representing 123 building-events (data points) were computed using System Identification methods. Building height ranges from 30 ft to 168.8 ft, *PGA* ranges from 0.003g to 0.453g, *PGV* ranges from 0.161cm/s to 54.904 cm/s, and *PGD* ranges from 0.008cm to 13.778cm. Our recommended regression equation for estimating the fundamental period, and first mode damping of RCMRF buildings is given in Eqs. (3) and (4). Comparison of regression results for T_1 at *PGV*=10cm/s and ASCE 7-10 formula are shown in Figure 5. The 95% confidence and prediction intervals for the equation presented for first modal damping are presented in Figure 6.

$$T_1 = 0.01H^1 PGV^{0.12} \quad \text{Eq. (3)}$$

$$\xi_1 = 3.89\, PGV^{0.05} \quad \text{Eq. (4)}$$

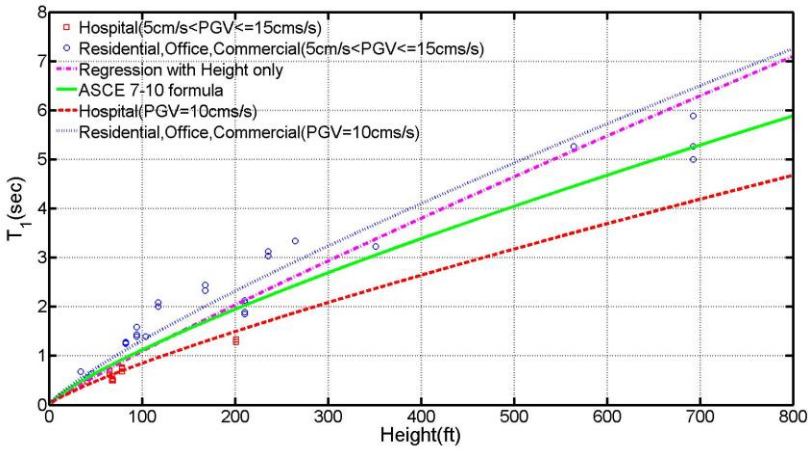

Figure 3. Fundamental period for SMRF buildings regressed on Height vs. ASCE 7-10 formula

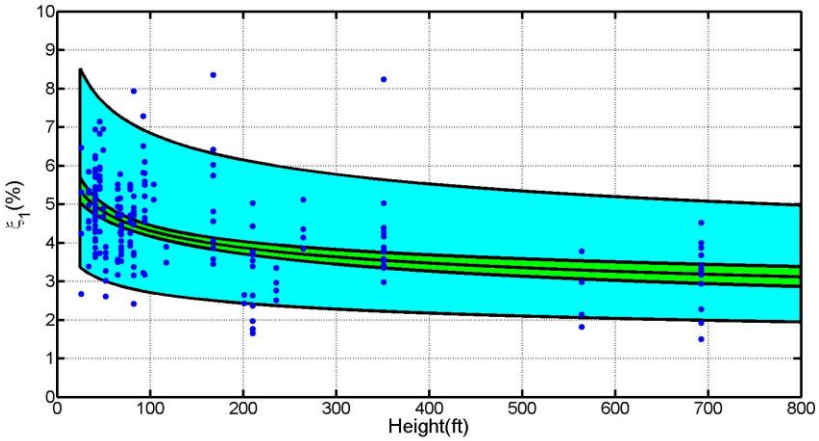

Figure 4. 95% confidence and prediction range for first mode equivalent damping of SMRF

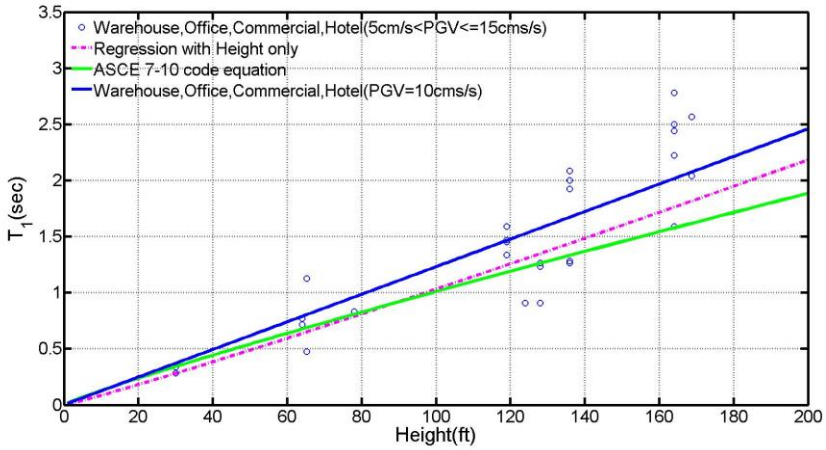

Figure 5. Fundamental period for RCMRF buildings regressed on Height vs. ASCE 7-10 formula

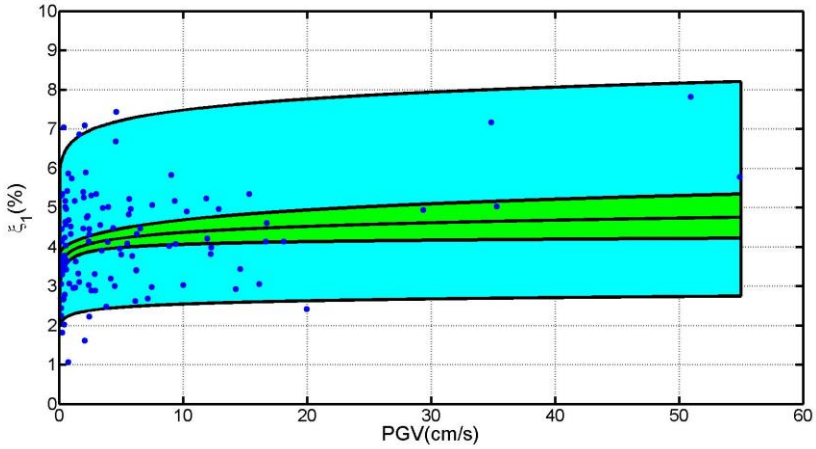

Figure 6. 95% confidence and prediction range for first mode equivalent damping of RCMRF

Modal Properties and for Reinforced Concrete Walls (RCW)

Thirty RCW buildings, with heights ranging from 27.5 ft. to 229.33 ft, representing 336 building-events (data points) were used for quantifying their dynamic properties. *PGA*, *PGV*, and *PGD* range from 0.001g to 0.798g, 0.062cm/s to 112.139 cm/s, and 0.003cm to 28.298cm, respectively. The buildings were divided into two subcategories: (1) Library, Residential, Office, Hotel, Commercial buildings and Parking Structures, and (2) Schools and Hospitals. Recommended equations for T_1 and ξ_1 of RCW buildings is given in Eqs. (5) & (6). Comparison of regression results for *PGV*=10cm/s and ASCE 7-10 formula are shown in Figure 7. The 95% confidence and prediction intervals for the regression equation are presented in Figure 8.

$$T_1 = \begin{cases} 0.009H^{0.87}PGV^{0.02} & \text{School/Hospital} \\ 0.013H^{0.87}PGV^{0.02} & \text{Other} \end{cases} \qquad \text{Eq. (5)}$$

$$\xi_1 = 5.06H^{-0.08} \qquad \text{Eq. (6)}$$

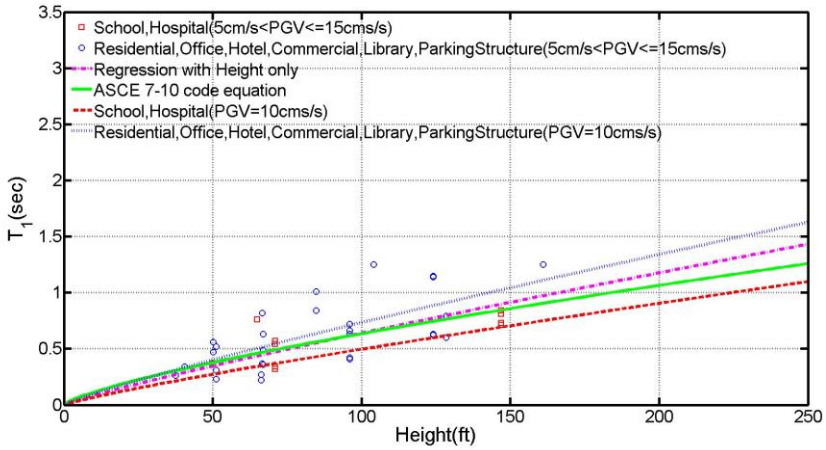

Figure 7. Fundamental period for RCW buildings regressed on Height vs. ASCE 7-10 formula

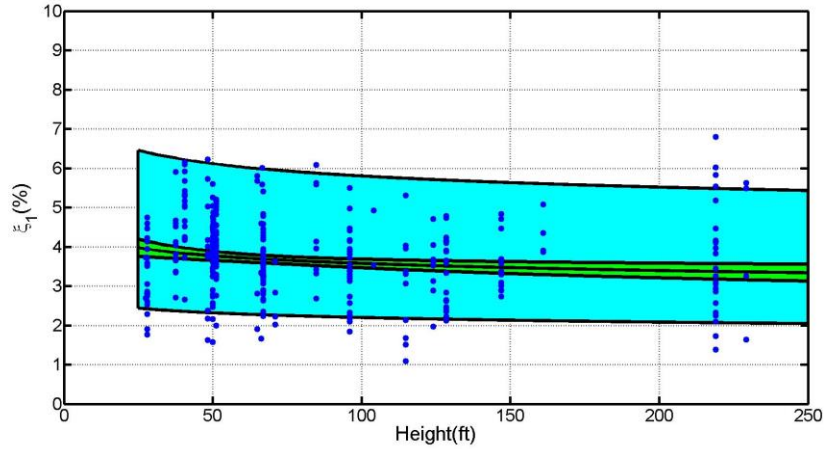

Figure 8. 95% confidence and prediction range for first mode equivalent damping of RCW

Modal Properties and for Concentrically Braced Frames (CBF)

Dynamic properties of 11 CBF buildings representing 144 building-events were computed; 31.92' < *H* < 716', 0.001g < *PGA* < 0.327g, 0.001 cm/s< *PGV* < 29.640cm/s, and 0.003cm < *PGD* < 9.813cm. The buildings were divided into two subcategories: (1) Industrial, Office, Commercial buildings and Parking Structures, and (2) Jails and Hospitals. The recommended equations for T_1 and ξ_1 of CBF buildings is given in Eqs. (7) & (8). Comparison of regression results and ASCE 7-10 formula are shown in Figure 9. The 95% confidence and prediction intervals for the regression equation are presented in Figure 10.

$$T_1 = \begin{cases} 0.005H^{1.02} & \text{Jail/ Hospital} \\ 0.007H^{1.02} & \text{Other} \end{cases} \qquad \text{Eq. (7)}$$

$$\xi_1 = 3.37 \qquad \text{Eq. (8)}$$

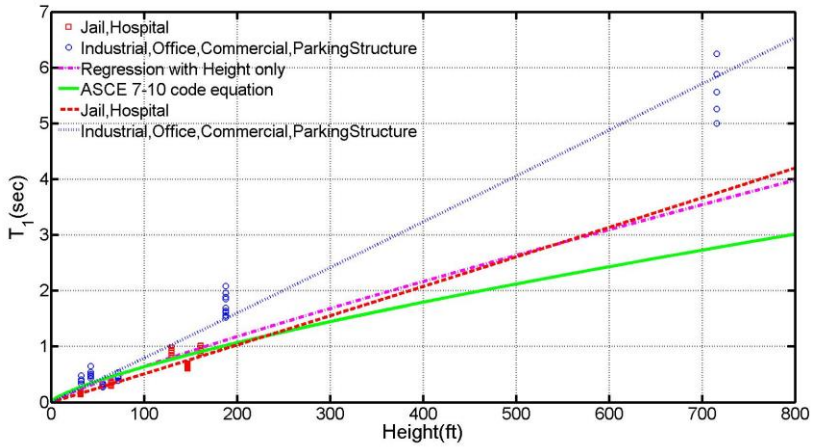

Figure 9. Fundamental period for CBF buildings regressed on Height vs. ASCE 7-10 formula.

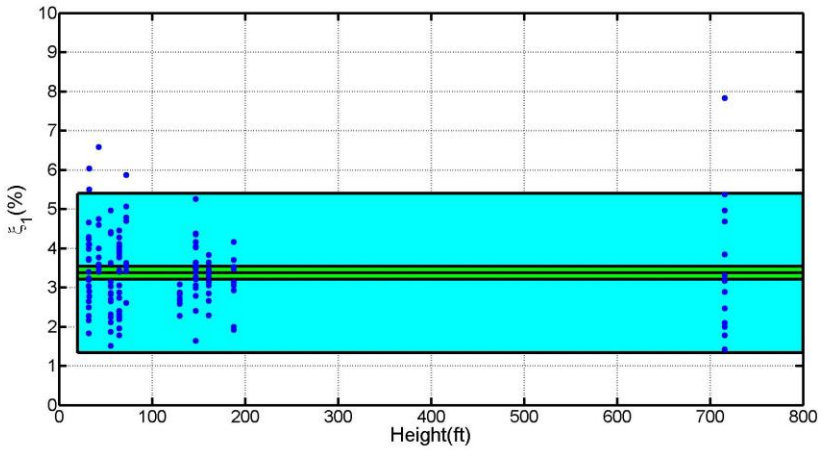

Figure 10. 95% confidence and prediction range for first mode equivalent damping of CBF

Modal Properties and for Eccentrically Braced Frames (EBF)

11 EBF buildings representing 144 building-events were used to generate equations for their fundamental period and first modal damping; see Eqs. (9) & (10). Building height ranges from 31.92ft to 716 ft, *PGA* ranges from 0.001g to 0.327g, *PGV* ranges from 0.001cm/s to 29.640 cm/s, and *PGD* ranges from 0.003cm to 9.813cm. The buildings were divided into two subcategories: (1) Industrial, Office, Commercial buildings and Parking Structures, and (2) Jails and Hospitals. Comparison of regression results and ASCE 7-10 formula are shown in Figure 9. The 95% confidence and prediction intervals for the regression equation are presented in Figure 10.

$$T_1 = 0.07 H^{0.46} PGV^{0.04} \qquad \text{Eq. (9)}$$

$$\xi_1 = 6.43 H^{-0.13} \qquad \text{Eq. (10)}$$

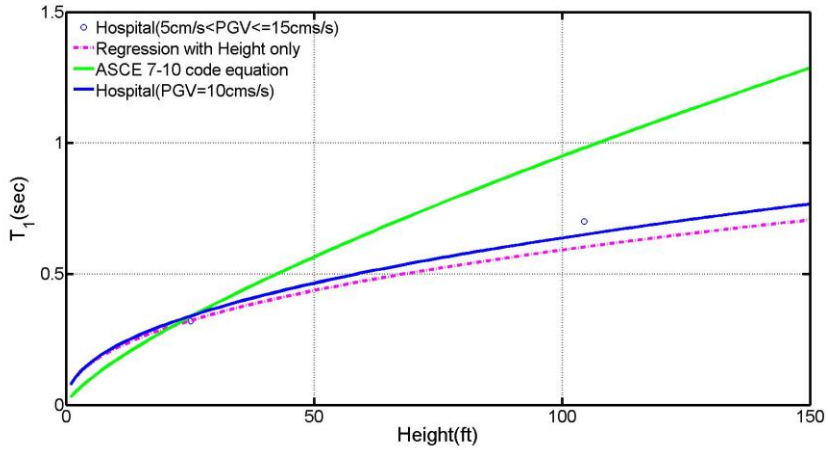

Figure 11. Fundamental period for EBF buildings regressed on Height vs. ASCE 7-10 formula.

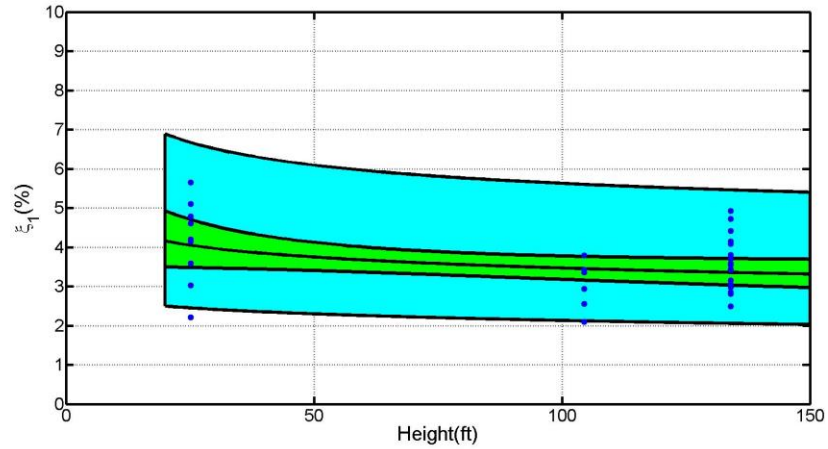

Figure 12. 95% confidence and prediction range for first mode equivalent damping of EBF

Modal Properties and for Masonry Walls (MAW)

Eqs. (11) & (12) show our suggested formulation for T_1 and ξ_1 of MAWs. 5 MAW buildings representing 72 building-events were utilized with building height ranges from 22ft to 85ft. Data point suggest a *PGA* range between 0.002g to 0.258g, *PGV* range between 0.091cm/s to 33.003cm/s, and *PGD* range from 0.006cm to 7.900cm. Comparison of regression results and ASCE 7-10 formula are shown in Figure 13. The 95% confidence and prediction intervals for the regression equation are presented in Figure 14.

$$T_1 = 0.004\,H^{1.09} \qquad \text{Eq. (11)}$$

$$\xi_1 = 3.62 \qquad \text{Eq. (12)}$$

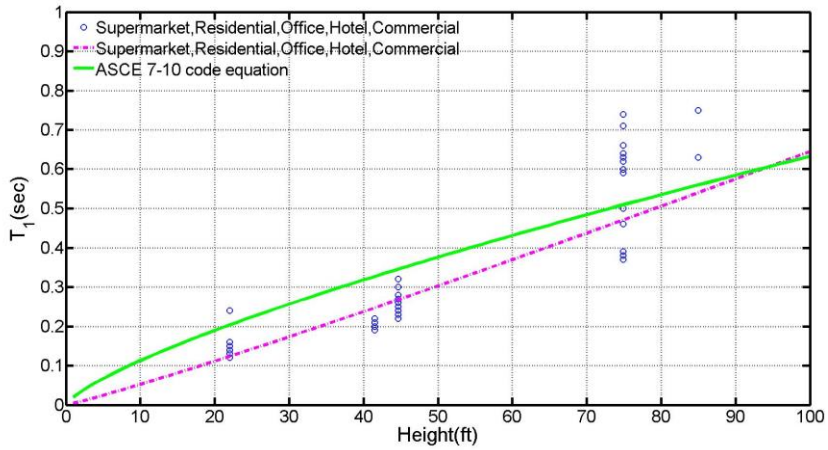

Figure 11. Fundamental period for MAW buildings regressed on Height vs. ASCE 7-10 formula.

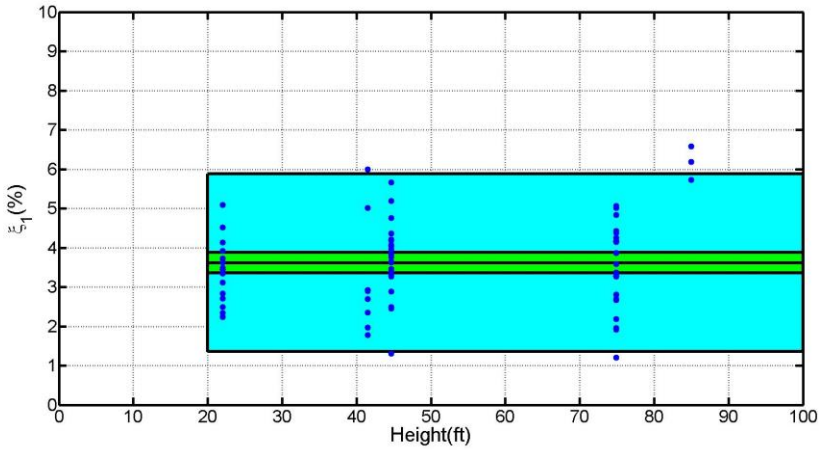

Figure 12. 95% confidence and prediction range for first mode equivalent damping of MAW

Acknowledgements

The contents of this report were developed under Agreement No. 1014-962 from the California Department of Conservation, California Geological Survey, Strong Motion Instrumentation Program. However, these contents do not necessarily represent the policy of that agency nor endorsement by the State Government.

References

ATC (1978). Tentative provisions for the development of seismic regulations for buildings. *Rep. No. ATC 3-06*, Applied Technological Council, Palo Alto, Calif.

Amanat, K. M., & Hoque, E. (2006). A rationale for determining the natural period of RC building frames having infill. *Engineering Structures*, **28**(4), 495-502.

ASCE-American Society of Civil Engineers (2010). *Minimum Design Loads for Buildings and Other Structures* (ASCE/SEI 7–10). American Society of Civil Engineers: Reston, VA.

Bentz, A., & Kijewski-Correa, T. (2008). Predictive models for damping in buildings: the role of structural system characteristics. In *Proceedings of the 2008 Structures Congress, 18th Analysis and Computation Specialty Conference, Vancouver, Canada*.

Bernal, D. (1994). Viscous damping in inelastic structural response. *ASCE Journal of Structural Engineering*, **120**(4): 1240-1254.

Bernal, D., Mozaffari Kojidi, S., Kwan, K., & Döhler, M. (2012). Damping identification in buildings from earthquake records. *SMIP12 Seminar on Utilization of Strong-Motion Data, p. 39 - 56.*

Cole, E. E., Tokas, C. V., & Meehan, J. F. (1992). Analysis of recorded building data to verify or improve 1991 Uniform Building Code (UBC) period of vibration formulas. *Proc. SMIP92. Strong Motion Instrumentation Program, Division of Mines and Geology, California Department of Conservation*. Sacramento, Calif.

Davenport, A. G., & Hill-Carroll, P. (1986). Damping in tall buildings: its variability and treatment in design. In *Building motion in wind*, p. 42-57. ASCE.

Fang, J. Q., Jeary, A. P., Li, Q. S., & Wong, C. K. (1999). Random damping in buildings and its AR model. *Journal of Wind Engineering and Industrial Aerodynamics*, **79**(1), 159-167.

Federal Emergency Management Agency (FEMA), 2012. *Seismic Performance Assessment of Buildings Volume 1 – Methodology, Tech. Rep. P-58-1*, Washington, D.C.

Ghahari, S.F., Abazarsa, F., Ghannad, M.A., Celebi, M., & Taciroglu, E. (2014). Blind modal identification of structures from spatially sparse seismic response signals. *Earthquake Engineering and Structural Dynamics*, **21**(6): 649-674.

Goel, R., & Chopra, A.K. (1997). "Period formulas for moment-resisting frame buildings". *Journal of Structural Engineering*; **123**(11): 1454 – 1461.

Goel, R., & Chopra, A.K. (1998). "Period formulas for concrete shear wall frame buildings". *Journal of Structural Engineering*; **124**(4): 426 – 433.

Hatzigeorgiou, G. D., & Kanapitsas, G., 2013. Evaluation of fundamental period of low-rise and mid-rise reinforced concrete buildings. *Earthquake Engineering & Structural Dynamics*, **42**(11), 1599-1616.

Hong, L. L., & Hwang, W. L. (2000). Empirical formula for fundamental vibration periods of reinforced concrete buildings in Taiwan. *Earthquake engineering & structural dynamics*, **29**(3), 327-337.

Jeary, A. P. (1997). Damping in structures. *Journal of Wind Engineering and Industrial Aerodynamics*, 72: 345 – 55.

Kocak, A., & Yildirim, M. K. (2011). Effects of Infill Wall Ratio on the Period of Reinforced Concrete Framed Buildings. *Advances in Structural Engineering* **14**(5), 731-744.

Kutner, M. H., Nachtsheim, C.J., Neter, J., & Li, W. (2005). *Applied Linear Statistical models*. Fifth Edition.

Kwon, O. S., & Kim, E. S. (2010). Evaluation of building period formulas for seismic design. *Earthquake Engineering & Structural Dynamics*, **39**(14), 1569-1583.

Lagomarsino, S. (1993). Forecast models for damping and vibration periods of buildings. *Journal of Wind Engineering and Industrial Aerodynamics*, **48**(2), 221-239.

Lee, L. H., Chang, K. K., & Chun, Y. S. (2000). Experimental formula for the fundamental period of RC buildings with shear-wall dominant systems. *The Structural Design of Tall Buildings*, **9**(4), 295-307.

Li, Q. S., Liu, D. K., Fang, J. Q., Jeary, A. P., & Wong, C. K. (2000). Damping in buildings: its neural network model and AR model. *Engineering Structures*, **22**(9), 1216-1223.

Ljung, L. (1999) *System Identification: Theory for the User*, Upper Saddle River, NJ, Prentice-Hal PTR.

LATBSDC (2014). *An Alternative Procedure for Seismic Analysis and Design of Tall Buildings Located in The Los Angeles Region.* Los Angeles Tall Buildings Structural Design Council.

Luş, H., Betti, R., & Longman, R. W. (1999). Identification of linear structural systems using earthquake induced vibration data. *Earthquake Engineering and Structural Dynamics*, 28:1449-1467.

Memari, A. M., Aghakouchak, A. A., Ashtiany, M. G., & Tiv, M., (1999). Full-scale dynamic testing of a steel frame building during construction, *Engineering Structures*, **21**(12), 1115-1127.

NCHRP (1994). *Recommended Provisions for the Development of Seismic Regulations for New Buildings*, National Earthquake Hazards Reduction Program, Building Seismic Safety Council.

Poovarodom, N., & Charoenpong, K., 2008. Identification of Dynamic Properties of Low-Rise RC Building by Ambient Vibration Measurements During Construction, in *Proceedings, 14th World Conference on Earthquake Engineering*, 12–17 October, 2008, Beijing, China.

Meeting of the Architectural Institute of Japan (AIJ), p. 379-380.

Satake, N., Suda, K. I., Arakawa, T., Sasaki, A., & Tamura, Y. (2003). Damping evaluation using full-scale data of buildings in Japan. *Journal of structural engineering*, **129**(4), 470-477.

Skolnik, D., Yu, E., Wallace, J., & Taciroglu, E. (2007). Modal System Identification & Finite Element Model Updating of a 15-story Building using Earthquake & Ambient Vibration Data. *In Structural Engineering Research Frontiers*, p. 1-14. ASCE.

SEAOC (1988). *Recommended Lateral Force Requirements,* Structure Engineers Association of California, Seismology Committee.

SEAOC (1990). *Recommended Lateral Force Requirements,* Structure Engineers Association of California, Seismology Committee.

SEAOC (1996). *Recommended Lateral Force Requirements,* Structure Engineers Association of California, Seismology Committee.

Tamura, Y., & Yoshida, A. (2008). Amplitude dependency of damping in buildings. In *Proceedings of the 18th Analysis and Computation Specialty Conference* (Vol. 315).

UBC (1991). International Conference of Building Officials, *Uniform Building code*, 1991 Edition.

UBC (1997). International Conference of Building Officials, *Uniform Building code*, 1997 Edition.

Van Overschee, P., & De Moor, B. (1994). N4SID: Subspace algorithms for the identification of combined deterministic-stochastic systems. *Automatica*, **30**(1), 75-93.

Wyatt, T. A. (1977, May). Mechanisms of damping. In *Proceeding of a Symposium of Dynamic Behavior of Bridges at the Transpor and Road Research Laboratory, Crowthorne, Berkshire, England, May 19, 1977*. (No. TRRL Rpt. 275 Proceeding).

Appendix A

Table A.1. Set of buildings used in this study

Index	Building Station	Primary VLLR	Building Height (ft)	Number of Stories	Number of Eqs X Dir
1	12299	SMRF	65.5	4	8
2	13312	SMRF		13	10
3	14323	SMRF	104.0	7	2
4	14533	SMRF	265.0	15	6
5	23481	SMRF	94.4	7	10
6	23515	SMRF	117.6	9	2
7	23516	SMRF	41.3	3	18
8	23634	SMRF	69.0	5	10
9	24104	SMRF	41.0	2	16
10	24198	SMRF	34.0	2	8
11	24288	SMRF	351.2	32	16
12	24370	SMRF	82.5	6	14
13	24566	SMRF	168.0	12	12
14	24569	SMRF	236.0	15	4
15	24609	SMRF	78.5	5	8
16	24629	SMRF	692.5	54	14
17	54388	SMRF	26.0	2	4
18	57357	SMRF	210.6	13	12
19	57562	SMRF	49.5	3	4
20	58261	SMRF	52.5	4	6
21	58354	SMRF	201.1	13	4
22	58506	SMRF	46.2	3	12
23	58532	SMRF	564.0	47	4
24	58755	SMRF	92.5	6	4
25	68669	SMRF	67.9	4	6
26	12493	RCMRF	64.0	4	12
27	23511	RCMRF	30.0	3	20
28	24322	RCMRF	164.0	13	14
29	24386	RCMRF	65.2	7	15
30	24454	RCMRF	39.0	4	2
31	24463	RCMRF	119.0	5	18
32	24464	RCMRF	168.8	20	8
33	24571	RCMRF	136.0	9	12
34	24579	RCMRF	128.0	10	14
35	57355	RCMRF	124.0	10	6
36	58490	RCMRF	78.0	6	2
37	12267	RCW	48.3	4	10
38	12284	RCW	50.2	4	20
39	13329	RCW		8	6
40	13589	RCW	146.9	11	14
41	13620	RCW	27.5	2	2
42	14311	RCW	71.0	5	4
43	23285	RCW	67.0	5	28
44	23287	RCW	51.1	6	36
45	24514	RCW	96.0	6	10
46	24655	RCW	67.0	6	12
47	24680	RCW	161.0	14	4

48	25339	RCW	114.9	12	12
49	47459	RCW	66.3	4	4
50	57355	RCW	124.0	10	7
51	57356	RCW	96.0	10	15
52	58224	RCW	28.0	2	24
53	58334	RCW		3	20
54	58337	RCW		11	16
55	58348	RCW	40.6	3	20
56	58364	RCW	128.5	10	22
57	58394	RCW	104.0	9	2
58	58462	RCW	84.8	6	8
59	58479	RCW	65.0	6	6
60	58480	RCW	229.3	18	4
61	58483	RCW	219.0	24	24
62	58488	RCW	50.0	4	10
63	58503	RCW	37.5	3	12
64	68387	RCW	66.7	5	2
65	68489	RCW	124.0	14	2
66	89770	RCW	50.0	4	24
67	13698	CBF	42.5	2	8
68	13702	CBF	161.0	7	12
69	14654	CBF	188.0	14	10
70	24248	CBF	147.0	9	22
71	24332	CBF	72.5	5	8
72	24602	CBF	716.0	57	14
73	24713	CBF	130.0	8	8
74	47796	CBF	65.0	3	24
75	54331	CBF	31.9	2	18
76	57948	CBF	32.5	2	5
77	58196	CBF	55.8	5	16
78	24249	EBF	134.0	8	18
79	57594	EBF	104.5	5	6
80	58496	EBF	25.2	3	10
81	23544	MAW	85.0	6	3
82	24232	MAW	50.0	4	2
83	24517	MAW	41.5	3	8
84	58492	MAW	74.9	8	22
85	89473	MAW	22.0	1	16
86	89494	MAW	44.7	5	23
87	24385	PCW	88.0	10	20
88	24601	PCW	149.7	17	6
89	58639	PCW	114.0	13	14
90	23540	RCTUW	29.0	2	1
91	57502	RCTUW	31.6	2	8
92	24541	URM	82.1	6	8
93	12759	WOOD	12.3	2	12
94	36531	WOOD	13.2	2	6